Conference materials
UDC 535-15
DOI: https://doi.org/10.18721/JPM.153.256

Photoluminescent α-$NaYbF_4$:$Er_{0.02}Ce_{0.02}Zn_{0.1}$ nanoparticles for bioimaging in visible and infrared ranges

E. M. Trifanova ✉, A. V. Koshelev, K. V. Khaydukov, I. V. Krylov, V. K. Popov

Federal Scientific Research Center "Crystallography and Photonics" RAS, Moscow, Russia

✉ katikin@mail.ru

Abstract. Nowadays noninvasive optical technologies require multifunctional nanomarkers, that can perform photoluminescence in different ranges of spectrum to provide broad possibilities for bioimaging. Photoluminescent nanoparticles doped with rare earth elements meet these requirements and are very promising for biological tissue visualization. **α**-$NaYbF_4$:$Er_{0.02}Ce_{0.02}Zn_{0.1}$ nanoparticles were characterized, had narrow and intensive photoluminescent peaks. Experiments were carried out on visualization in the visible and IR ranges of the spectrum. It was shown that a long photoluminescence lifetime made it possible to use the method of time-gated luminescence imaging. Visualization experiments with phantoms of biotissue both 3.5% fat milk and distilled water showed that nanoparticles can be used for multipurpose bioimaging.

Keywords: Photoluminescent nanoparticles, bioimaging, biotissue transparency windows, time-gated luminescence imaging

Funding: The study was funded by the Ministry of Science and Higher Education of the Russian Federation within the State Assignment FSRC 'Crystallography and Photonics' of RAS and RFBR, Project 20-32-90218.

Citation: Trifanova E. M., Koshelev A. V., Krylov I. V., Khaydukov K. V., Popov V. K., Photoluminescent α-$NaYbF_4$:$Er_{0.02}Ce_{0.02}Zn_{0.1}$ nanoparticles for bioimaging in visible and infrared ranges, St. Petersburg State Polytechnical University Journal. Physics and Mathematics. 15 (3.2) (2022) 306–310. DOI: https://doi.org/10.18721/JPM.153.256

Материалы конференции
УДК 535-15
DOI: https://doi.org/10.18721/JPM.153.256

Фотолюминесцентные наночастицы α-$NaYbF_4$:$Er_{0,02}Ce_{0,02}Zn_{0,1}$ для биоимиджинга в видимом и инфракрасном диапазонах

Е. М. Трифанова ✉, А. В. Кошелев, К. В. Хайдуков, И. В. Крылов, В. К. Попов

Федеральный научно-исследовательский центр "Кристаллография и фотоника" РАН, г. Москва, Россия

✉ katikin@mail.ru

Аннотация. В настоящее время для неинвазивных оптических технологий требуются многофункциональные наномаркеры, способные люминесцировать в различных диапазонах спектра, что обеспечивает широкие возможности для биоимиджинга. Фотолюминесцентные наночастицы, легированные ионами редкоземельных элементов, отвечают этим требованиям и весьма перспективны для визуализации биологических тканей. Наночастицы α-$NaYbF_4$:$Er_{0,02}Ce_{0,02}Zn_{0,1}$, демонстрирующие интенсивную фотолюминесценцию в широком спектральном диапазоне, выбраны в качестве объекта исследования. Эксперименты по визуализации в видимом и ИК-диапазонах спектра сквозь сильно рассеивающую среду (3,5% цельное коровье молоко) и дистиллированную воду показали, что наночастицы α-$NaYbF_4$:$Er_{0,02}Ce_{0,02}Zn_{0,1}$ могут быть использованы для мультифункционального биоимиджинга.

Ключевые слова: Фотолюминесцентные наночастицы, биоимиджинг, окна прозрачности биотканей, фотолюминесцентная визуализация с отложенной регистрацией сигнала

Финансирование: Работа выполнена при поддержке Министерства науки и высшего образования в рамках выполнения работ по Государственному заданию ФНИЦ «Кристаллография и фотоника» РАН и РФФИ (проект № 20-32-90218_Аспиранты).

Ссылка при цитировании: Трифанова Е. М., Кошелев А. В., Крылов И. В., Хайдуков К. В., Попов В. К.Фотолюминесцентные наночастицы α-$NaYbF_4$:$Er_{0.02}Ce_{0.02}Zn_{0.1}$ для биоимиджинга в видимом и инфракрасном диапазонах // Научно-технические ведомости СПбГПУ. Физико-математические науки. Т. 15. № 3.2. С. 306–310. DOI: https://doi.org/10.18721/JPM.153.256

Introduction

Noninvasive optical technologies including NIR and SWIR regions of spectrum usually use three biotissue transparency windows (BTW): I-BTW (650–950 nm), II-BTW (1000–1350 nm), III-BTW (1500–1870 nm) for bioimaging. Biological tissue has deeper penetration depths according to local minimum of loss coefficient in these wavelength ranges compared with visible range of spectrum [1]. Technologies that use I-BTW and III-BTW attract significant interest due to high signal-to-noise ratio, high spatial and time resolution [2]. Biological tissues have different compositions, but almost all of them consist water [3]. Water has a high absorption coefficient in III-BTW, which can complicate visualization at these wavelengths [4]. Therefore, to implement bioimaging in several BTWs at once, depending on optical properties of a biological object under study, it is important to develop universal multimodal nanomarkers with several photoluminescence peaks in a wide spectral range. Inorganic fluoride nanocrystals, doped with lanthanide (Ln^{3+}) ions, demonstrated the required spectral characteristics [5]. Compared with other luminophores (quantum dotes, fluorescent dyes and proteins) Ln^{3+} doped fluoride nanoparticles (NPs) have a number of advantages for bioimaging applications [6]. They demonstrate superior chemical and photostability, narrow band and large luminescence shifts relative to excitation light [7]. Depending on the specific application, the luminescence characteristics of fluoride NPs can be varied by changing the nature of the host lattice and doping elements. NPs $NaYbF_4$, co-doped with Er^{3+} and Ce^{3+} can be used in fast in vivo brain imaging in the IR region above 1500 nm [8]. Temperature dependent NIR emission band pairs in II-BTW and III-BTW can be received by doping $NaGdF_4$ NPs with Ho^{3+}/Nd^{3+} or Er^{3+}/Nd^{3+} [9]. $NaYF_4$ nanocrystals doped with Yb^{3+} and Tm^{3+} ions have been successfully used for bioimaging of the ovarian cancer cells line at the wavelength of $\lambda = 800$ nm corresponding to I-BTW [10]. Also, presence of a large number of metastable long-lived excited 4f-states of Ln^{3+} ions makes it possible to use such NPs for time-gated luminescence imaging. In the context of noninvasive optical technologies this method allows the laser excitation signal and autoluminescence with a short lifetime to decay before the signal from the NPs with a long lifetime is received [11].

In this work, we demonstrated the possibility of using Ln^{3+}-doped α-$NaYbF_4$ NPs, which exhibit high intensity up- (~650 nm) and down-conversion (~1530 nm) photoluminescence under $\lambda = 976$ nm irradiation, as imaging instrument. Two visualization experiments were carried out: imaging through a strongly scattering medium (3.5% fat cow milk) and distilled water aiming to imitate scattering and absorption coefficient of biotissue. Our experiments showed broad perspective in multipurpose visualization with photoluminescent NPs and recommendations on the choice of the detecting range depending on specificity of the application.

Materials and Methods

Lanthanide doped α-$NaYbF_4$:$Er_{0.02}Ce_{0.02}Zn_{0.1}$ NPs were synthesized by thermolysis method. The phase composition of the obtained nanocrystals was studied using an X-ray powder diffractometer Rigaku Miniflex 600 (radiation CuKα) in the range of angles $10° \le 2\theta \le 120°$ with 1° scan step. The phases were identified using the ICDD PDF-2 (2014). The unit-cell parameters were calculated by the Le Bail full-profile fitting (the Jana2006 software). A semiconductor ATC-laser

with radiation peak at λ = 976 nm (Semiconductor Devices, Russia) was used to excite the NPs. The study of photoluminescence spectrum of NPs was carried out on a spectrofluorimeter Fluorolog 3 (HJY, France). The photoluminescence lifetime was measured under excitation of the semiconductor laser in a pulsed mode. The excitation laser beam was divided by splitter ~20/80%. 20% went on a silicon photodetector APDF and the rest 80% - on photomultiplier (PMT, Hamamatsu, Japan). The PMT signal corresponding to the decay kinetics was recorded on a TDS 6804B high-speed oscilloscope (Tektronix Inc., United States). TEM analysis was performed on a Tecnai Osiris (FEI, Hillsboro, OR, USA) electron microscope operated at 200 kV.

Experimental samples were prepared as follows: two pieces (1x10 mm) of white paper were covered with the NPs. The paper pieces were placed on a quartz cuvette with a 0.7 mm gap between them. 3.5% fat cow milk was chosen as a strongly scattering medium and distilled water was chosen as a medium with high absorption coefficient at λ = 1530 nm [4]. Quartz cuvettes with optical paths length of 1−11 mm were used for experiments with distilled water.

For visualization in the visible range, we used a custom-build imaging system with EMCCD camera (Raptor Photonics Incorporated, USA). PC with the software controlled laser galvanometer scanner (Ateco Technocenter, Russia) for precise aiming of the laser beam on the sample. The system of interference filters (Semrock, USA) was used to notch the exciting radiation off. For visualization in the IR range, we performed time-gated luminescence imaging, using InGaAs camera (Hamamatsu, Japan). A chopper wheel was controlled by MC2000B optical light modulator (Thorlabs, USA) and installed between the InGaAs camera and the sample. The laser was in a pulsed mode.

Results and Discussion

The XRD analysis results of α-$NaYbF_4$:$Er_{0.02}Ce_{0.02}Zn_{0.1}$ NPs are shown in Fig. 1a. The reflections on the X-ray diffraction pattern correspond to the cubic structure of α-$NaYbF_4$ (space group $Fm\bar{3}m$, a = 5.469(6) Å). According to the TEM data, the obtained nanocrystals were monodisperse particles of irregular shape with an average size of 36 nm (Fig. 1,*b*).

The photoluminescent properties of NPs are due to successive absorption of photons by ytterbium ions and further resonant nonradiative energy transfer to erbium ions within the crystalline matrix. The photoluminescence spectrum of NPs is shown in Fig. 2,*a*. The spectrum exhibits luminescence peaks in the visible and IR ranges of the spectrum, which correspond to characteristic electronic transitions in Er^{3+} ion. Yb^{3+} ions populate the $^2F_{5/2}$ excited state during absorption of IR radiation at λ = 976 nm. Then this ion nonradiatively transfers this energy to closely spaced neighboring Er^{3+}. The Er^{3+} ions populate the metastable $^4I_{11/2}$ excited state, where it can participate in synchronous energy exchange with the neighboring excited Yb^{3+}, so that Er^{3+} populate higher energy levels $^4F_{7/2}$ and $^2G_{7/2}$. From an excited states $^2H_{9/2}$, $^2H_{11/2}$/$^4S_{3/2}$, $^4F_{9/2}$ it passes into a state $^4I_{15/2}$ with the emission of photons with λ = 407, 525, 540, 652 nm respectively. When interacting with Ce^{3+}, a resonant population of levels of Er^{3+} occurs above $^4I_{13/2}$. As a result, the NPs have an intense luminescence peak at λ = 1530 nm (Fig. 2,*b*). We measured the photoluminescence lifetime. At λ = 1530 nm, it is 5.7 ms, which is suitable for time-gated photoluminescence imaging.

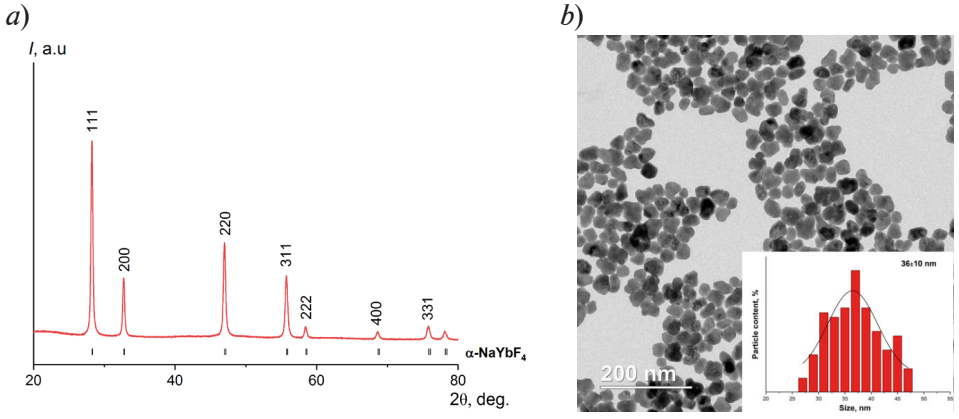

Fig. 1. X-ray diffraction pattern (*a*), TEM images and histograms of size distribution of α-$NaYbF_4$:$Er_{0.02}Ce_{0.02}Zn_{0.1}$ nanoparticles (*b*)

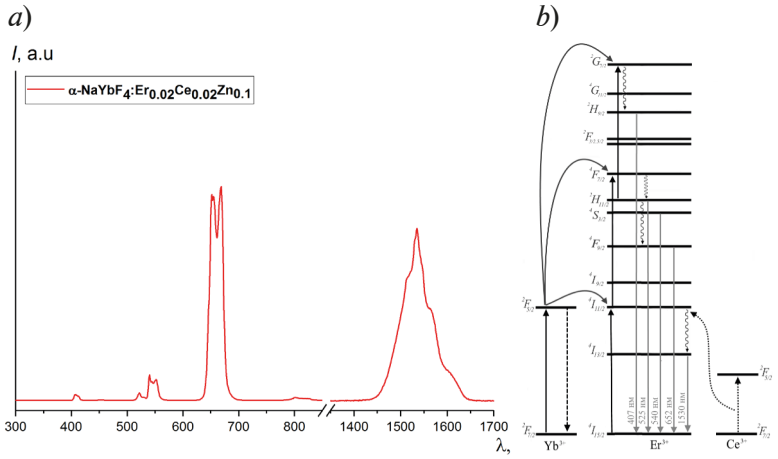

Fig. 2. Photoluminescence spectrum (*a*) energy level diagram of α-$NaYbF_4$:$Er_{0.02}Ce_{0.02}Zn_{0.1}$ nanoparticles (*b*)

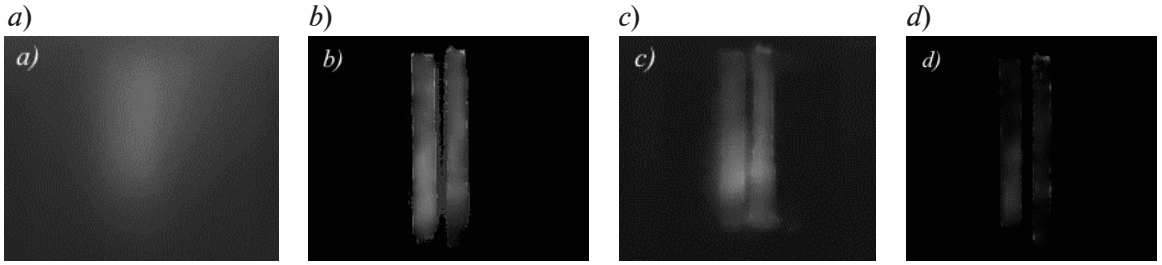

Fig. 3. Images of the samples obtained through a 1 mm layer of 3.5% fat milk in visible (*a*) and NIR (*b*) region and through a 4 mm layer of water in visible (*c*) and NIR (*d*) region

We obtained images of samples in the visible and IR ranges of the spectrum through 1 mm layer of 3.5% fat cow milk. In the first case gap between the pieces is not observed, it is impossible to separate the image of one paper band from the other (Fig. 3,*a*). In contrast to the image obtained at λ = 1530 nm (Fig. 3,*b*). The two luminescent bands are clearly visible. This can be explained by the Mie scattering effect – greater the wavelength, less light is scattered [12].

Several experiments were carried out with distilled water. The results are shown in Fig. 3,*c* and 3,*d*. The thickness of the water layer was increased from 1 mm to 11 mm. After 4 mm layer of water, the image in the IR range disappears. This is due to the high absorption coefficient of water at λ = 1530 nm ~10^3 cm^{-1}, while at λ = 652 it is only ~10^{-2} cm^{-1} [4]. In the visible range the image is preserved up to a layer 11 mm thick, the gap is clearly visible in all images.

Conclusion

Various visualization tasks sometimes require individual solutions. Therefore, it is so important to find universal multifunctional nanomarkers performing photoluminescent radiation in different ranges of the spectrum. Clear images of NPs were α-$NaYbF_4$:$Er_{0.02}Ce_{0.02}Zn_{0.1}$ on the surface the paper pieces obtained through media with different optical properties. It was shown that for visualization through a strongly scattering medium, the time-gated photoluminescence imaging in IR region of the spectrum was perfectly suitable due to the long photoluminescence lifetime (more than 5 ms) of the NPs. While the experiment with increasing the thickness of the water layer showed that there was a strong absorption of radiation at λ = 1530 nm. Therefore, it is possible to conduct through a medium with a high water content at λ ≤ 700 nm. The α-$NaYbF_4$:$Er_{0.02}Ce_{0.02}Zn_{0.1}$ NPs can be used as multipurpose photoluminescent nanomarkers both in I-BTW and III-BTW region of the spectrum.

Acknowledgments

The study was funded by the Ministry of Science and Higher Education within the State assignment FSRC 'Crystallography and Photonics' RAS and RFBR according to the project 20-32-90218. The authors are grateful to D.N. Karimov, and E.V. Khaydukov for fruitful discussions.

REFERENCES

1. **Hemmer E., Venkatachalam N., Hyodo H., Hattori A., Ebina Y., Kishimoto H., Soga K.,** Upconverting and NIR emitting rare earth based nanostructures for NIR-bioimaging, Nanoscale. 5 (23) (2013) 11339.

2. **Hemmer E., Benayas A., Légaré F., Vetrone F.,** Exploiting the biological windows: Current perspectives on fluorescent bioprobes emitting above 1000 nm, Nanoscale Horizons. 1 (3) Royal Society of Chemistry, (2016) 168–184.

3. **Bachmann L., Zezell D.M., Ribeiro A. da C., Gomes L., Ito A.S.,** Fluorescence Spectroscopy of Biological Tissues—A Review, Applied Spectroscopy Reviews. 41 (6) (2006) 575–590.

4. **Beć K.B., Huck C.W.,** Breakthrough Potential in Near-Infrared Spectroscopy: Spectra Simulation. A Review of Recent Developments, Frontiers in Chemistry. 7 (FEB) (2019) 1–22.

5. **Zhong Y., Dai H.,** A mini-review on rare-earth down-conversion nanoparticles for NIR-II imaging of biological systems, Nano Research. 13 (5) (2020) 1281–1294.

6. **Cheng L., Yang K., Zhang S., Shao M., Lee S., Liu Z.,** Highly-sensitive multiplexed in vivo imaging using pegylated upconversion nanoparticles, Nano Research. 3 (10) (2010) 722–732.

7. **Zhou J., Liu Z., Li F.,** Upconversion nanophosphors for small-animal imaging, Chem. Soc. Rev. 41 (3) (2012) 1323–1349.

8. **Zhong Y., Ma Z., Zhu S., Yue J., Zhang M., Antaris A.L., Yuan J., Cui R., Wan H., Zhou Y., Wang W., Huang N.F., Luo J., Hu Z., Dai H.,** Boosting the down-shifting luminescence of rare-earth nanocrystals for biological imaging beyond 1500 nm, Nature Communications. 8 (1) Springer US, (2017) 737.

9. **Skripka A., Benayas A., Marin R., Canton P., Hemmer E., Vetrone F.,** Double rare-earth nanothermometer in aqueous media: Opening the third optical transparency window to temperature sensing, Nanoscale. 9 (9) Royal Society of Chemistry, (2017) 3079–3085.

10. **Boyer J.-C., Manseau M.-P., Murray J.I., van Veggel F.C.J.M.,** Surface Modification of Upconverting NaYF 4 Nanoparticles with PEG–Phosphate Ligands for NIR (800 nm) Biolabeling within the Biological Window, Langmuir. 26 (2) (2010) 1157–1164.

11. **Khaydukov E. V., Boldyrev K.N., Khaydukov K. V., Krylov I. V., Asharchuk I.M., Savelyev A.G., Rocheva V. V., Karimov D.N., Nechaev A. V., Zvyagin A. V.,** Deferred Registration of Nanophosphor Photoluminescence As a Platform for Optical Bioimaging, Optics and Spectroscopy. 126 (1) (2019) 95–101.

12. **Mie G.,** Sättigungsstrom und Stromkurve einer schlecht leitenden Flüssigkeit, Annalen der Physik. 331 (8) (1908) 597–614.

THE AUTHORS

TRIFANOVA Ekaterina
katikin@mail.ru
ORCID: 0000-0003-4320-6917

KHAYDUKOV Kirill
haidukov_11@mail.ru
ORCID: 0000-0001-5898-2404

KOSHELEV Alexander
avkoshelev03@gmail.com
ORCID: 0000-0002-2119-6992

POPOV Vladimir
popov@laser.ru
ORCID: 0000-0002-9305-6964

KRYLOV Ivan V.
ivan_krylov@bk.ru

Received 15.07.2022. Approved after reviewing 18.07.2022. Accepted 19.07.2022.